

## Finite Element Modeling, Analysis and Fatigue Life Prediction of Lower Suspension Arm

M. M. Rahman<sup>1</sup>, M. M. Noor<sup>1</sup>, K. Kadirgama<sup>1</sup>, Rosli A. Bakar<sup>1</sup>, M.R.M. Rejab<sup>1</sup>

**Abstract-** This paper explores the finite element modeling, analysis and fatigue life prediction of lower suspension arm using the strain-life approach. Aluminum alloys are selected as a suspension arm materials. The structural model of the suspension arm was utilizing the Solid works. The finite element model and analysis were performed utilizing the finite element analysis code. TET10 mesh and maximum principal stress were considered in the linear static stress analysis and the critical location was considered at node (6017). From the fatigue analysis, Smith-Watson-Topper mean stress correction was conservative method when subjected to SAETRN loading, while Coffin-Manson model is applicable when subjected to SAESUS and SAEBRKT loading. From the material optimization, 7075-T6 aluminum alloy is suitable material of the suspension arm.

*Keywords:* Lower Suspension arm, finite element analysis, variable amplitude loading, strain-life method, Aluminum alloy.

### I. INTRODUCTION

In automotive industry, aluminum (Al) alloy has limited usage due to their higher cost and less developed manufacturing process compared to steels. However, Al alloy has the advantage of lower weight and therefore has been used increasingly in car industry for the last 30 years, mainly as engine block, engine parts, brake components,

steering components and suspension arms where significant weight can be achieved [1]. The increasing use of Al is due to the safety, environmental and performance benefits that aluminum offers, as well as the improved fuel consumption because of light weight. One of the important structural limitations of an aluminum alloy is its fatigue properties. This study is aimed at the automotive industry, more specifically a wrought aluminum suspension system, where safety is of great concern. Most of the time to failure consists of crack initiation and a conservative approach is to denote the component as failed when a crack has initiated [2]. This simplification allows designers to use linear elastic stress results obtained from multibody dynamic FE (finite element) simulations for fatigue life analysis. The suspension arm is subjected to cyclic loading and it is consequently exposed to fatigue damage. In the suspension arm, uncertainty is related to loads expected given to the car component due to individual driving styles and road conditions. Therefore, the prediction of fatigue life is less accurate even under controlled laboratory conditions. Hence the numerical simulation is implemented because of cheap and easy to perform as well as provide insight to the mechanism [3]. Rahman et al. [3] were studied about finite element based durability assessment in a two- stroke free piston linear engine component using variable amplitude loading. Authors discussed the finite element analysis to predict the fatigue life and identify the critical locations of the component. The effect of mean stress on the fatigue life also investigated. The linear static finite element analysis was performed using MSC.NASTRAN. The result was capable of showing the contour plots of the fatigue life histogram and damage histogram at the most critical location. Conle and Mousseau [4] used the vehicle simulation and finite element result to generate the fatigue life contours for the chassis component using automotive proving ground load history result combine with the computational techniques. They concluded that the combination of the dynamics modeling, finite element analysis is the practical techniques for the fatigue design of the automotive component. Kim et al. [5] was studied a method for simulating vehicles dynamic loads, but they add durability. Nadot and Denier [6] have been studied fatigue phenomena for nodular cast iron automotive suspension arms. The authors found that the major parameter influencing fatigue failure of casting components are casting defects. The high cycle fatigue behaviour is controlled mainly by surface defects such as dross defects and oxides while the low cycle fatigue is governed by multiple cracks initiated independently from casting defects. Svensson et al. [7] was conducted the fatigue life prediction based on

<sup>1</sup>M. M. Rahman with the Automotive Excellence Center, Faculty of Mechanical Engineering, Universiti Malaysia Pahang, Tun Abdul Razak Highway, 26300 Kuantan, Malaysia (phone: +6-09-5492207, Fax: +6-09-5492244, E-mail: mustafizur@ump.edu.my).

<sup>1</sup>M.M. Noor with the Faculty of Mechanical Engineering, Universiti Malaysia Pahang, Tun Abdul Razak Highway, 26300 Kuantan, Malaysia (E-mail: muhamad@ump.edu.my).

<sup>1</sup>K. Kadirgama with the Faculty of Mechanical Engineering, Universiti Malaysia Pahang, Tun Abdul Razak Highway, 26300 Kuantan, Malaysia (E-mail: kumaran@ump.edu.my).

<sup>1</sup>Rosli Abu Bakar with the Faculty of Mechanical Engineering, Universiti Malaysia Pahang, Tun Abdul Razak Highway, 26300 Kuantan, Malaysia (E-mail: rosli@ump.edu.my).

<sup>1</sup>M.R.M.Rejab with the Faculty of Mechanical Engineering, Universiti Malaysia Pahang, Tun Abdul Razak Highway, 26300 Kuantan, Malaysia (E-mail: ruzaimi@ump.edu.my).

variable amplitude tests-specific applications. Three engineering components have been tested with both constant amplitude loading and different load spectra and the results are analyzed by means of a new evaluation method. The method relies on the Palmgren-Miner hypothesis, but offers the opportunity to approve the hypothesis validity by narrowing the domain of its application in accordance with a specific situation. In the first case automotive spot weld components are tested with two different synthetic spectra and the result is extrapolated to new service spectra. Molent et al. [8] was evaluated the spectrum fatigue crack growth using variable amplitude data. This paper summarizes a recent semi-empirical model that appears to be capable of producing more accurate fatigue life predictions using flight load spectra based on realistic in-service usage. The main objective of this project is to conduct the finite element modeling, analysis and fatigue life prediction of aluminum alloy based suspension arm under variable amplitude loading. The overall objectives are to predict the fatigue life of suspension arm using strain-life method and identify the critical location; to optimize the material for the suspension arm.

## II. FINITE ELEMENT BASED FATIGUE ANALYSIS

Fatigue analysis has traditionally been performed at a later stage of the design cycle. This is due to the fact that the loading information could only be derived from the direct measurement, which requires a prototype [9]. Multibody dynamics is capable of predicting the component loads which enable designer to undertake a fatigue assessment even before the prototype is fabricated [3]. The purpose of analyzing a structure early in the design cycle is to reduce the development time and cost. This is achieved to determine the critical region of the structure and improving the design before prototype are built and tested. The finite element (FE) based on fatigue analysis can be considered as a complete engineering analysis for the component. The fatigue life can be estimated for every element in the finite element model, and the contour plots of life damage can be obtained. The geometry information is provided by the FE result for each load case applied independently. Appropriate material properties are also provided for the desired fatigue analysis method. An integrated approach to fatigue life analysis combines the multibody dynamic analysis, finite element analysis, and the fatigue analysis into a consistent entity for the prediction of the fatigue life of a component [3]. The flowchart of the finite element based fatigue analysis is shown in Figure 1.

### A. Material Information

Material model and material properties play an important role in the result of the FE method. The material properties are one of the major inputs which is the definition of how a material behaves under the cyclic loading conditions. The cyclic material properties are used to calculate the elastic-plastic stress-strain response and the rate at which fatigue damage accumulate due to each fatigue cycle. The materials parameters required depend on the analysis methodology being used. The mechanical properties of 6082-T6 aluminum alloy are shown in Table 1.

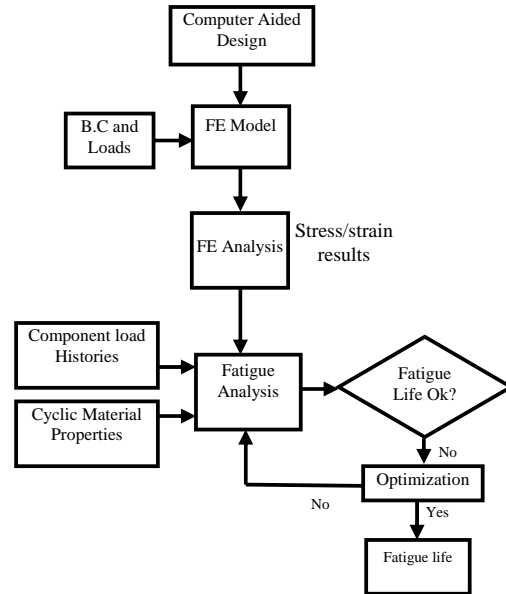


Figure 1. The finite element based fatigue analysis

Table 1. Mechanical properties of aluminum alloy 6082-T6

Properties	Aluminum alloy 6082-T6
<b>Monotonic Properties</b>	
Tensile strength, $\sigma_{UTS}$ (MPa)	330
Yield strength, $\sigma_{YS}$ (MPa)	307
Young's modulus, $E$ (GPa)	70
Elongation, $\epsilon_r$ (%)	9
<b>Cyclic and fatigue properties</b>	
Fatigue strength exponent, $b$	-0.07
Fatigue strength coefficient, $\sigma'_f$ (MPa)	486.8
Fatigue ductility exponent, $c$	-0.593
Fatigue ductility coefficient, $\epsilon'_f$	0.209

## III. STRAIN-LIFE METHOD

Fatigue analyses can be performed using either one of the three basic methodologies including the stress-life approach, strain-life approach, and crack growth approach. The stress-life method was first applied over a hundred years ago and considers nominal elastic stresses and how they are related to life. This approach to the fatigue analysis of components works well for situations in which only elastic stresses and strains are present. However, most components may appear to have nominally cyclic elastic stresses but stress concentrations present in the component may result in local cyclic plastic deformation. Under these conditions, the local strain-life method uses the local strains as the governing fatigue parameter. The strain-life approach can be used proactively for a component during early design stages. The local strain-life approach is preferred if the loading history is irregular and where the mean stress and the load sequence effects are thought to be of importance. The strain-life approach involves the techniques for converting the loading history, geometry and materials properties (monotonic and

cyclic) input into a fatigue life prediction. The operations involved in the prediction process must be performed sequentially. First, the stress and strain at the critical region are estimated and then the rainflow cycle counting method [10] is used to reduce the load-time history. The next step is to use the finite element method to convert the reduced load-time history into a strain-time history and also to calculate the stress and strain in the highly stressed area. Then, the crack initiation methods are employed to predict the fatigue life. The simple linear hypothesis proposed by Palmgren [11] and Miner [12] is used to accumulate the fatigue damage. Finally, the damage values for all cycles are summed until a critical damage sum (failure criteria) is reached.

The fatigue resistance of metals can be characterized by a strain-life curve. These curves are derived from the polished laboratory specimens tested under completely reversed strain control. The relationship between the total strain amplitude ( $\Delta\varepsilon/2$ ) and the reversals to failure ( $2N_f$ ) can be expressed in Eq. (1) [13-14]. The Coffin-Manson total strain-life is mathematically defined as in Eq. (1).

$$\frac{\Delta\varepsilon}{2} = \frac{\sigma'_f}{E} (2N_f)^b + \varepsilon'_f (2N_f)^c \quad (1)$$

where  $N_f$  is the fatigue life;  $\sigma'_f$  is the fatigue strength coefficient;  $E$  is the modulus of elasticity;  $b$  is the fatigue strength exponent;  $\varepsilon'_f$  is the fatigue ductility coefficient; and  $c$  is the fatigue ductility exponent.

In designing for the durability, the presence of nonzero mean stress normal stress can influence fatigue behaviour of materials due to a tensile or compressive normal mean stress. In conjunction with the local strain-life approach, many models have proposed to quantify the effect of mean stresses on fatigue behaviour. The commonly used models in the ground vehicle industry are those by Morrow [15] and by Smith, Watson, and Topper [16]. These two models are described in the following sections. Morrow [15] has proposed the following relationship when a mean stress is expressed in Eq. (2).

$$\varepsilon_a = \frac{\sigma'_f - \sigma_m}{E} (2N_f)^b + \varepsilon'_f (2N_f)^c \quad (2)$$

Equation (2) implies that the mean normal stress taken into account by modifying the elastic part of the strain-life curve by the mean stress ( $\sigma_m$ ).

Smith, Watson, and Topper [16] proposed another mean stress model which is called Smith- Watson-Topper (SWT) mean stress correction. It is mathematically defined in Eq. (3).

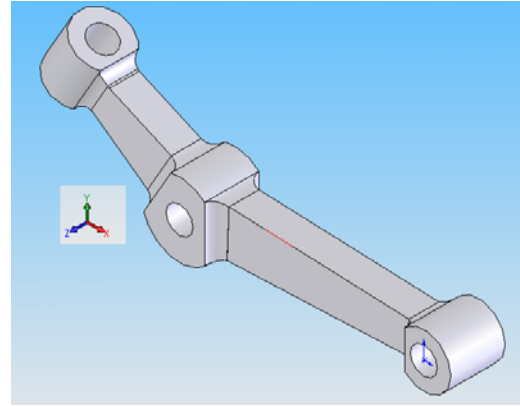
$$\sigma_{\max} \varepsilon_a E = (\sigma'_f)^2 (2N_f)^{2b} + \sigma'_f \varepsilon'_f E (2N_f)^{b+c} \quad (3)$$

where  $\sigma_{\max}$  is the maximum stress, and  $\varepsilon_a$  is the strain amplitude.

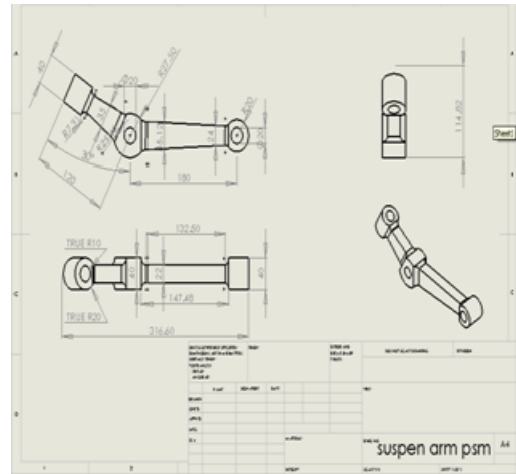
## IV. RESULTS AND DISCUSSION

### A. Finite Element Modeling

The suspension arm is one of the important components in the automotive suspension component. Therefore, constraints are used to specify the prescribed enforce displacement and to enforce rest condition in the specified direction at grid point reaction. A simple three-dimensional model of suspension arm was developed using SolidWorks software as shown in Figure 3. A 10 node tetrahedral element (TET10) was used for the solid mesh. Sensitivity analysis was performed to determine the optimum element size. These analyses were performed iteratively at different mesh global length until the appropriate accuracy obtained. Convergence of the stresses was recorded as the mesh global length was refined. The mesh global length of 0.3 mm was considered and the force 150 N was applied one end of the bushing that connected to the tire. The other two bushing that connected to the body of the car are constraint. These preload is based on Nadot and Denier [6]. The three-dimensional FE model, loading and constraints of suspension arm is shown in Figure 4.



(a) Structural Modeling



(b) Overall dimension

Figure 3: Structural model and overall dimensions of suspension arm

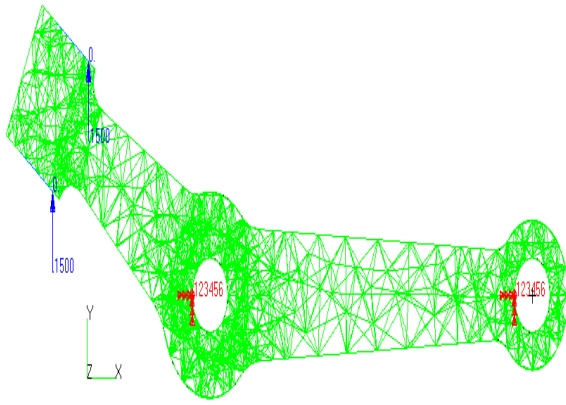
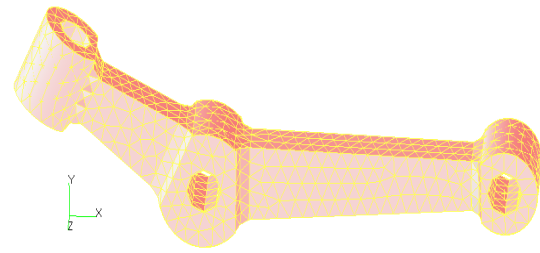


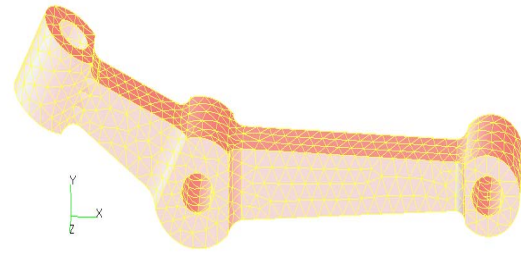
Figure 4. Three-dimensional FE model, loading and constraints.

### B. Influence of Mesh Type

Mesh study was performed on the FE model to refine the mesh for the accuracy of the calculated result depends on the competitive cost (CPU time). During the analysis, the specific variable and the mesh convergence was monitored and evaluated. The mesh convergence is based on the geometry, model topology and analysis objectives. For this analysis, the auto tetrahedral meshing approach is employed for the meshing of the solid region geometry. Tetrahedral meshing produce high quality meshing for boundary representation most of solids model imported from CAD systems. The tetrahedral elements (TET10) and tetrahedral elements (TET4) are used for the initial analysis based on the loading conditions (Figure 4). The finite element model using TET4 and TET10 type of elements as shown in Figure 5 and von Mises stress contour is shown in Figure 6 for TET4 and TET10 elements. Analysis shown that TET10 mesh predicted higher von Mises stress than the TET4 mesh (Figure 6) various mesh global length. Then, the comparison was made between these two elements based on von Mises, Tresca, maximum principal stresses and displacement are tabulated in Table 2 and 3 for TET 10 and TET4 respectively. According to the results from Table 2 and 3, it can be seen that the TET10 are able to capture the higher stresses compared to TET4 for the same mesh global length. Thus, TET10 is used for overall analysis. Variation of maximum principal stresses and displacement against the global mesh length are shown in Figure 7 and 8 respectively. It can be seen that the TET10 gives the higher stress and displacement throughout the global mesh length.

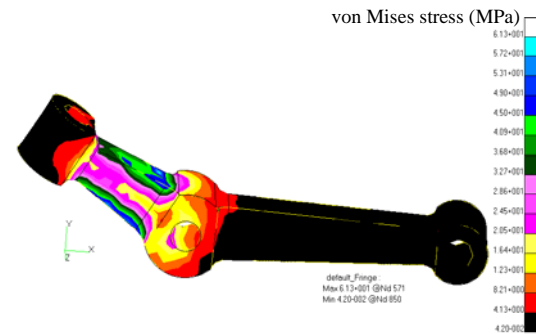


(a)

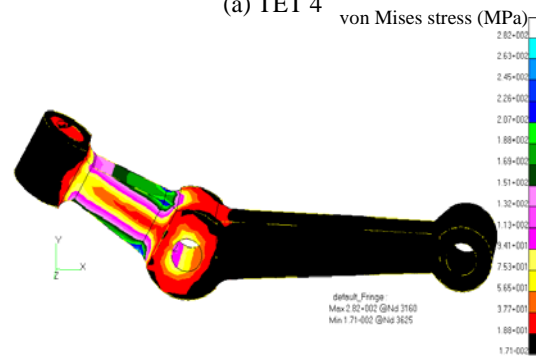


(b)

Figure 5 (a) TET4, 5559 elements and 1445 nodes; (b) TET10, 5576 elements and 9431 nodes



(a) TET 4



(b) TET 10

Figure 6. von Mises stresses contours (a) for TET4; (b) for TET10

Table 2. Variation of stresses at critical location for TET10 mesh.

Mesh Size (mm)	Total Nodes	Total Elements	von Mises (MPa)	Tresca (MPa)	max principal stress (MPa)	Displacement (mm)
0.3	9394	5549	386	394	397	0.054
0.8	7174	4182	374	381	392	0.056
1	6376	3710	363	373	379	0.056
1.3	4861	2761	334	345	363	0.047
1.5	4548	2548	282	289	290	0.039
2	1991	995	197	203	217	0.032

Table 3. Variation of stresses at critical location for TET4 mesh.

Mesh Size (mm)	Total nodes	Total Elements	von Mises (MPa)	Tresca (MPa)	max principal stress (MPa)	Displacement (mm)
0.3	1444	5546	69	72	75	0.013
0.8	1111	4169	60	62	60	0.012
1	987	3693	59	63	58	0.012
1.3	767	2742	50	53	52	0.010
1.5	719	2517	46	49	46	0.009
2	336	969	27	29	29	0.006

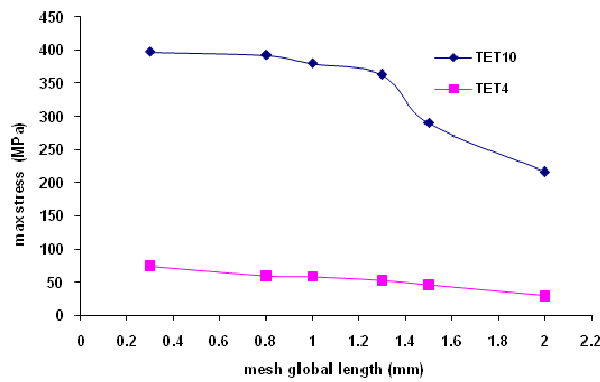


Figure 7. Variation of maximum principal stress for different element types

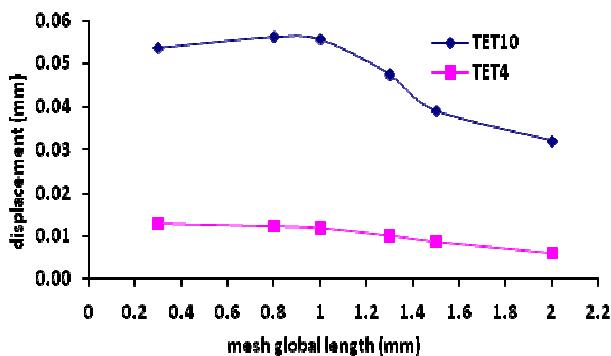


Figure 8. Variation of maximum displacement for different element type

### C. Identification of Mesh Convergence

The convergence of the stress was considered as the main criteria to select the mesh type. The finite element mesh was generated using the TET10 for various mesh

global length. Figure 9 shows the predicted results of stresses at the critical location of the suspension arm. It can be seen that the smaller the mesh size capture the higher predicted stresses. It is concluded from the figure that the maximum principal stresses is suitable for fatigue analysis. It can be seen that mesh size of 0.3 mm (5549 elements) has obtained the maximum stresses, which is almost flatter in nature. The mesh size smaller than 0.3 mm are not implemented due the limitation of computational time (CPU time) and storage capacity of the computer. Hence, the maximum principal stress based on TET10 at 0.3 mm mesh size is used in the fatigue life analysis since the stress is higher compared to Von Mises and Tresca principal stress.

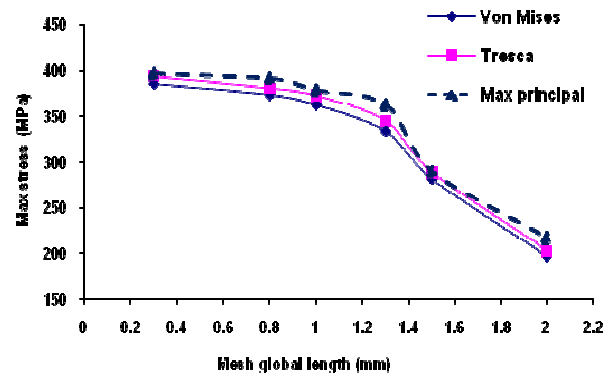


Figure 9. Stresses versus mesh size at critical location for TET10 to check mesh convergence.

### D. Linear Static Stress Analysis

The linear static stress analysis was performed utilizing MSC.NASTRAN to determine the stress and strain results from finite element model. The material models utilized of linear elastic and isotropic material. The choice of the linear elastic material model is compulsory. Model loading consists of the applied mechanical load which is

modeled as the load control and displacement control. The fillet of the bushing is found to experience the largest stresses. The result of the maximum principal stresses is used for the fatigue life analysis. The maximum principal stresses distributions of the suspension arm for the linear static stress analysis is shown in Figure 10 for 6082-T6 aluminum alloy. From the results, the maximum principal stresses of 397 MPa was obtained at node 6017.

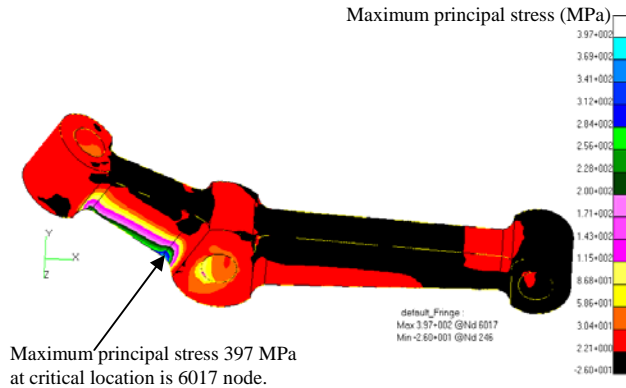


Figure 10. Maximum principal stresses contour plotted for 6082-T6 aluminum alloy with SAETRN loading.

#### E. Fatigue Analysis

The fatigue life of the suspension arm is initially predicted using 6082-T6 aluminum alloy with SAETRN loading using the strain-life method. This analysis is focused on the critical location at node 6017. The fatigue life is expressed in second for the variable amplitude loading. This analysis was performed to determine the fatigue life based on various variable amplitude loading time histories such as SAETRN (positive mean loading), SAESUS (negative mean loading) and SAEBKT (bracket mean loading) as given in Table 4. From Table 4, the fatigue life of the suspension at the critical location of node (1067) for various loading histories is different. The SAESUS loading histories gives the higher life compared to SAETRN and SAEBRKT loading histories. The distribution of fatigue life in term of log of life (sec) contour plotted for 6082-T6 aluminum alloy with SAETRN, loading histories are showed in Figure 11.

Table 4. Fatigue life at critical location of node (1067) for various loading histories for 6082-T6.

Loading histories	Fatigue life (seconds) $\times 10^4$		
	Coffin-Manson	Morrow	SWT
SAETRN	6.8	1.6	1.4
SAESUS	16.21	6.8	9.0
SAEBKT	0.14	2.4	2.7

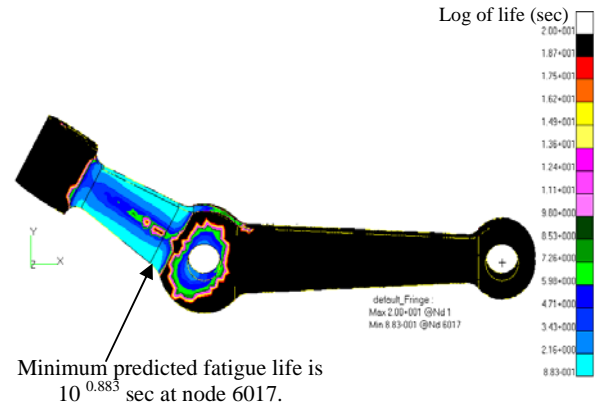


Figure 11. Predicted life contours plotted in term of log of life for 6082-T6 aluminum alloy with SAETRN loading.

#### V. CONCLUSION

From the analysis conducted, several conclusions can be drawn as follows.

- (i). Prediction of the fatigue life is focused on critical location of node 6017.
- (ii). SWT mean stress correction is conservative method when subjected to SAETRN loading histories while Coffin-Manson model is applicable in SAESUS and SAEBKT loading histories.
- (iii). No design modification is made on structural model of the suspension arm
- (iv). 7075-T6 is suitable material compared to others material in the optimization.

For further research, the experimental works under controlled laboratory conditions should be done to determine the validation of the result from the software analysis. Besides, the dimension of the structural model of the suspension arm should be modified to get the significant result during the experiment. 7075-T6 aluminum alloy should be considered as the suitable material for the fabrication of the suspension arm.

#### ACKNOWLEDGMENT

The authors would like to thank Universiti Malaysia Pahang for provides laboratory facilities and financial support

#### REFERENCES

- [1] Kyrre, S.A. 2006. Fatigue life prediction of an alluminium alloy automotive component using finite element analysis of surface topography. PhD Thesis Dissertation. Norwegian University of Science and Technology Department of Structural Engineering.
- [2] Kyrre, S.A., Skallerud, B., Tveiten, W.T. and Holme, B. 2005. Fatigue life prediction of machined components using finite element analysis of surface topography, International Journal of Fatigue. 27: 1590- 1596

- [3] Rahman, M.M., Ariffin, A.K., Abdullah, S. and Jamaludin, N. 2007. Finite element based durability assessment of a free piston linear engine component. *SDHM*, 3 (1): 1-13
- [4] Conle, F.A and Mousseau, C.W. 1991. Using vehicle dynamic simulation and finite element result to generate fatigue life contours for chassis component. *International Journal of Fatigue* 13 (3): 195 - 205.
- [5] Kim, H.S, Yim, H.J and Kim, C.M. 2002. Computational durability prediction of body structure in prototype vehicles. *International Journal of Automotive Technology* 3 (4): 129-136
- [6] Nadot, Y. and Denier, V. 2003. Fatigue failure of suspension arm: experimental analysis and multiaxial criterion. *International journal of Fatigue*, 11 (4): 485 – 499.
- [7] Svensson, T., Johannesson, P. and Mare´a, J.D. 2005. Fatigue life prediction based on variable amplitude tests—specific applications. *International Journal of Fatigue*, 27: 966–973.
- [8] Molent, L., McDonald, M., Barter, S. and Jones, J. 2007. Evaluation of spectrum fatigue crack growth using variable amplitude data. *International Journal of Fatigue*, 30 (1): 119-137
- [9] Stephens, R.I, Fatemi, A., Stephens, R.R. & Fuchs, H.O. 2000. *Metal fatigue in engineering*. New York: John Wiley & Sons, Inc.
- [10] Matsuishi, M. and Endo, T. 1968. Fatigue of metals subjected to varying stress. Presented to JSME, Fukuoko, Japan.
- [11] Palmgren, A., 1924. Durability of ball bearings. *ZVDI*, 68(14): 339-341.M.
- [12] Miner, A., 1945. Cumulative damage in fatigue. *Journal of Applied Mechanics* 12: 159-164.
- [13] Coffin, L.F. 1954. A study of the effects of cyclic thermal stresses on a ductile metal. *Transactions of American Society for Testing and Materials* 76: 931-950.
- [14] Manson, S.S. 1953. Behavior of materials under conditions of thermal stress. *Heat Transfer Symposium*, pp. 9-75.
- [15] Morrow, J. 1968. *Fatigue Design Handbook: Advances in Engineering*. Warrendale, PA: SAE, 21-29
- [16] Smith, K.N., Watson, P. and Topper, T.H. 1970. A stress-strain functions for the fatigue on materials. *Journal of Materials*. 5 (4): 767-78.